The Effect of Pitch Angle Amplitudes on a Cyclorotor Performance Using Computational Fluid Dynamics

Wishchayapas Piluck [1], Kitsada Sangnak [1], Anaswee Arbubaka [1], and Teerawat Klabklay [2,*]

[1] Department of Power Engineering Technology, College of Industrial Technology, King Mongkut's University of Technology North Bangkok, 1518 Pracharad I Rd., Bangsue, Bangkok 10800, Thailand
[2] Research Centre for Combustion Technology and Alternative Energy—CTAE and College of Industrial Technology, King Mongkut's University of Technology North Bangkok, Bangkok 10800, Thailand
Email: s6503024621029@email.kmutnb.ac.th (W.P.); s6503024611015@email.kmutnb.ac.th (K.S.); s6503024621258@email.kmutnb.ac.th (A.A.); teerawat.k@cit.kmutnb.ac.th (T.K.)
*Corresponding author

***Abstract*—Currently, multirotor Unmanned Aerial Vehicles (UAVs) typically use propellers rotating around a vertical axis. However, the cyclorotor is a type of multirotor that the propellers rotate around the lateral axis. This configuration offers advantages such as increased compactness, stiffness, and safety compared to conventional rotors. This article focuses on studying the aerodynamic behavior of cyclorotors. The objective of this article is to study the effect of pitch angle amplitudes on the lift, propulsive force, torque, and lift-to-drag ratio using 2D Computational Fluid Dynamics (CFD) simulation. The variables of this study were as follows: the pitch angle amplitudes of 25º, 35º, 45º and the rotor speeds consisted of 400, 500, 600, 700, and 800 RPM. As a result, (i) The pitch angle amplitude of 45 degrees provided the highest lift of 29.717 N at 800 RPM. (ii) The pitch angle amplitude of 45º produced the maximum propulsive force of 11.026 N at 800 RPM. (iii) The pitch angle amplitude of 25º offered the lowest torque of 0.239 N.m at 400 RPM. (iv) The pitch angle amplitude of 25º s promoted the highest lift-to-torque ratio of 12.705 at 800 RPM.**

***Keywords*—cyclorotor, computational fluid dynamics, unmanned aerial vehicle**

I. Introduction

The Unmanned Aerial Vehicle (UAV) or Drone is considered a popular device that has been used for many applications in the world. It can also perform a variety of missions. There are 3 types of UAV namely, fixed wing, multirotor wing and fixed-wing hybrid. The multirotor wing is now the most popular. The problem with the use of the conventional multirotor is that rotating wings is quite dangerous, especially the high-speed rotation of the sharp wingtips extending outward from body. Furthermore, the conventional multirotor is not very compact and rigid. The cyclorotor is a type of multirotor propeller that the rotor blades rotate around the lateral axis [1, 2]. The pitch angle of each blade can change systematically according to the azimuth angles. The cyclorotor UAVs may help to fix these problems because their rotors rotate in lateral axis and are covered by protection guard at both side of rotors as shown in Fig. 1, so that it is safer while operating. Additionally, the advantage of cyclorotor type of UAV is more compact and stiffer including easier storage. This article focuses on studying the aerodynamic behavior of cyclorotors. The objective of this article is to study the effect of pitch angle amplitudes on the lift, propulsive force, torque, and lift-to-torque ratio by using the 2D Computational Fluid Dynamics (CFD) simulation. The variables of this study were as follows: the pitch angle amplitudes of 25º, 35º, 45º and the rotor speeds consisted of 400, 500, 600, 700, and 800 RPM. The 2-dimensional CFD simulation was implemented to analyze the turbulent flow by using the unsteady Reynolds-Averaged Navier-Stokes (URANS) and the k-ω SST turbulence model.

Fig. 1. A cyclorotor [3].

The researchers who have studied the fluid-dynamic efficiency of cyclorotor are as follows: Hu *et al.* [4] used the method of grid separation method with 2D unstable

Manuscript received March 5, 2025; revised March 19, 2025; accepted May 27, 2025; published September 8, 2025.

Reynolds average to maximize efficiency and significantly reduce interference between the blades. As a result, when the azimuth angle was variable, the large advance coefficient was likely to cause the highly turbulent pulse of the flow field structure to intensify at the large azimuth angle, which leads to more severe fluctuations in the driving force. Habibnia and Pascoa [5] studied the performance characteristics of cyclorotor-truster that can be used in the UAV, especially in the take-off and landing process. The result was that the distance of the aircraft had a great influence on performance and functionality in creating a wide thrust. Hu *et al.* [6] presented a numerical simulation model based on Unsteady Reynolds-Averaged Navier–Stokes equations (URANSs) results. The effects of blade aspect ratio and taper ratio were analyzed. The result showed that the cyclorotor with the same chord length had quite similar performance even though the blade aspect ratio varies from a very small value to a large one. By comparing the cycloidal rotors with different taper ratios, it was found that the rotors with large blade taper ratio outperform those with small taper ratio. This was because the blade with larger taper ratio had longer chords. Saito and Kurose [7] used Large-Eddy Simulation (LES) to study the effect of the interaction between the blades and the vortex at the blade tips on the aerodynamic performance of the cyclorotor. Focusing on a cyclorotor consisting of NACA0010 blades, which rotate at a speed of 800 RPM with a maximum angle of attack of 20º and considering the effect of the vortex at the blade tips. Additionally, the effect of the number of blades was studied by conducting LES on cyclorotors with blade counts ranging from 3 to 10 to determine the optimal number of blades. The simulation results of the cyclorotor with 6 blades showed good agreement with the experimental results and demonstrated that the vortices at the blade tips help increase the thrust generated by the blades on the windward side, particularly near the blade tips. Additionally, it was found that when the number of blades exceeds 7, the thrust generated by each blade significantly decreases, and the total thrust begins to decline. Xisto *et al.* [8] investigates the impact of blade geometry—specifically blade thickness and number of blades—on the performance of a cycloidal rotor (CROP) using unsteady Computational Fluid Dynamics (CFD). The results show that increasing blade thickness improves thrust and reduces power consumption by minimizing flow separation. Additionally, the optimal number of blades depends on the blade pitch angle; too many blades lead to aerodynamic interference and reduced efficiency.

II. Material and Methods

A. Validation Process

The validation process was first carried out to ensure that the results from simulation were accurate. The experimental data researched by Hu *et al.* [6] was used to compare with the simulation results from 2D CFD simulation technique which is the same method used in the current study. Hu *et al.* [6] studies the impact of aspect ratio and taper ratio on the hovering performance of cyclorotors. The difference between aspect ratio and taper ratio does not significantly impact performance, so more importance should be placed on airfoil and pitch angle. The procedure in brief for validation may be divided into 4 steps as follows: (i) create the geometry of the cyclorotor blade as illustrated in Fig. 2 by using data as shown in Table I, (ii) create the domain and suitable mesh for calculation as illustrated in Fig. 3, (iii) calculate using the numerical method of CFD technique, and (iv) gather all numerical and graphic results to discuss and conclude. The validation results would be mentioned in Section IV.A.

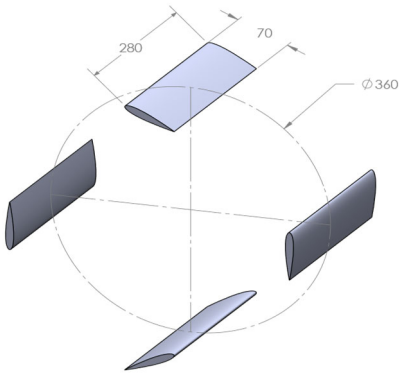

Fig. 2. Geometry of a cyclorotor for validation.

TABLE I. Cyclorotor Blade Data from the Research of Hu *et al.* [6]

Parameter	Value
Rotor diameter (mm)	360 mm
Number of blades	4 blades
Chord length (mm)	70 mm
Blade aspect ratio	4
Airfoil of blade	NACA0015
Blade pitch axis position	50% chord length from leading edge
Pitch angle amplitude (°)	45°

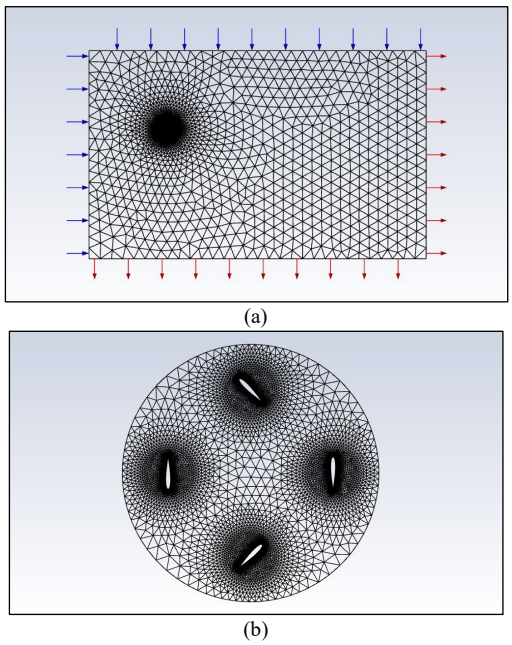

(a)

(b)

Fig. 3. Domain and mesh generation for validation: (a) Overall domain, (b) Rotating domain.

B. CFD Simulation Procedure

The geometry of the cyclorotor blade was modeled in 2D in a single rotor using SolidWorks. The 2D analysis is used because the chord length and pitch angle along blade span are constant. The authors assume 3D effect such as tip loss is not very much. Therefore, simplification with 2D analysis to estimate the trend of results can be preliminarily implemented. The results of 2D analysis would be calculated into 3D results by multiplying the length of blade to be able to compare the experiment. The rotor diameter was 360 ms with 4 blades in the shape of NACA0015 airfoil. The chord was 70 ms. The pitch angle could oscillate according to the azimuth angles. The pivot point of pitch oscillation was in the middle of chord. All this information was presented in Table II. The pitch angle amplitudes were 25º, 35º, and 45º as shown in Fig. 4. The domain and mesh were created using Fluid Flow Fluent in Workbench as illustrated in Figs. 4 and 5. The calculation with numerical method was implemented by Ansys Fluent in Workbench under the operation, boundary, and initial conditions as prescribed in Tables III and IV.

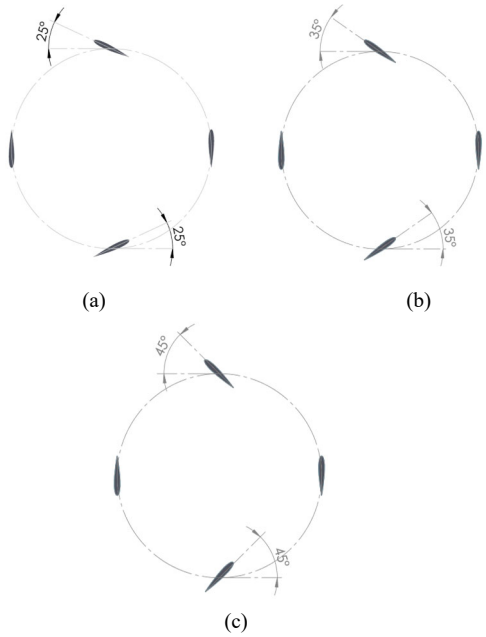

Fig. 4. The pitch angle amplitudes of the cyclorotor: (a) 25º, (b) 35º, (c) 45º.

TABLE II. GEOMETRY INFORMATION OF A SINGLE ROTOR FOR THIS STUDY

Parameter	Value
Rotor diameter (mm)	360 mm
Number of blades	4 blades
Chord length (mm)	70 mm
Pitch angle amplitude	25°, 35°, 45°
Pivot point	50%
Airfoil of blade	NACA0015

1) Domain and mesh preparation

The domain and mesh preparation are an important process for CFD simulation. Normally, the size of the domain must be approximately about 5–10 times (or more) larger than the size of the object being studied [9]. This study used 30, 100, 30, and 100 times of the rotor diameter for the above, below, left side, and right side, respectively, as shown in Fig. 5. It is obvious that the domain size at the right side and below of the rotor, which are the area of flow outlet, is longer than the above and the left side of the rotor, which are the area of flow inlet, because these two areas were a place where commonly appeared the strong turbulence. Mesh configuration must be suitable for those physical problems. For example, the near wall area of all blades must be created inflation mesh as shown in Fig. 5 so that the behavior of boundary layer existing on such area could be captured. The y^+ of the first layer of inflation was 4.41. The tetrahedral and structured mesh was created for this study by using Ansys Fluent 2024. As a result, the number of elements was about 80,000. Due to limited computer resources and the need for small time steps used for solving transient problems, the author attempted to optimize the grid refinement with limited element sizes as mentioned before.

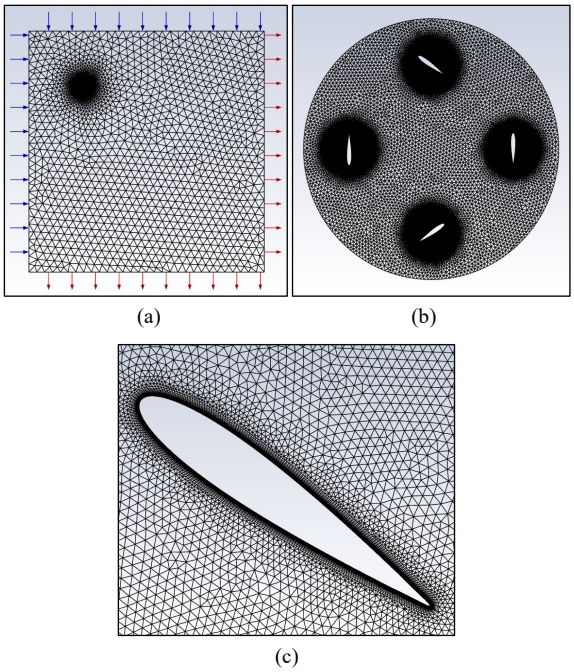

Fig. 5. Domain and mesh generation. (a) overall domain; (b) rotating domain; (c) inflation mesh.

TABLE III. OPERATION AND BOUNDARY CONDITIONS

Parameter	Value
Velocity inlet	0 m/s
Pressure outlet	0 bar (Guage pressure)
Wall	Moving wall
Rotation speed	400–800 RPM

TABLE IV. OPERATION MATERIAL PROPERTIES AND INITIAL CONDITIONS

Parameter	Value
Density	1.225 kg /m^3
Viscosity	1.789×10^{-5} kg·m/s
Time step size	0.001875–0.00375
Residual error	0.0001

III. Theory

A. Basics Information of Cyclorotor

The cyclorotor comprises a set of rotors placed in the radius of rotation [1, 2]. The position of each blade on the circumference is represented by the azimuth angle (ψ) and the pitch angles (β) of each blade can change systematically according to the azimuth angles as shown in Fig. 6. It is obvious that the time for changing that pitch angles depends on the speed of rotors. Therefore, the pitch angle is a function of time and azimuth angles, as expressed in Eq. (1). The center of pitch angle oscillation is called a pivot point, which is located on the chord line. This study uses pivot point of 50% of chord.

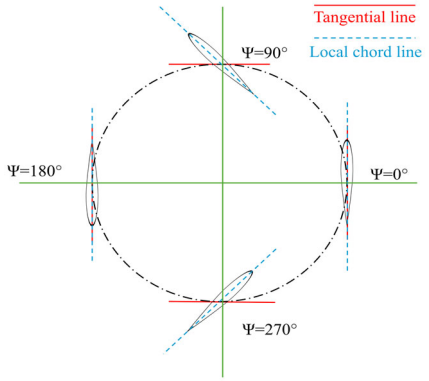

Fig. 6. Schematic diagram of a cyclorotor.

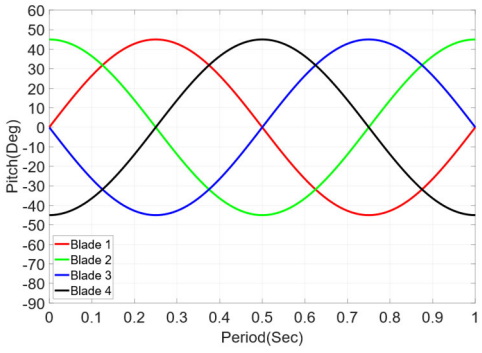

(a)

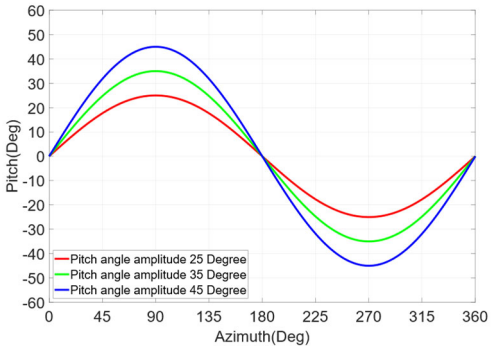

(b)

Fig. 7. The magnitude and oscillation of pitch angles: Blade Pitch Angle: (a) Time period of each blade of 45 Deg Pitch Amplitude; (b) Azimuth Position of blade 1.

The magnitudes of pitch angles for each blade at any azimuth as illustrated in Fig. 7 can be written as expressed in Eq. (1)

$$\beta = A\,sin(\omega \Delta t + \psi_i) \tag{1}$$

where β is the local pitch angle, A is the pitch angle amplitude, ω is the rotational speed of a rotor, Δt is the time step, and ψ_i is initial azimuth angle.

B. Computational Fluid Dynamics

The governing equations to analyze the turbulent flow are the partial differential equation consisting of continuity equation and Reynolds-Average Navier-Stroke (RANS) equation [10] as expressed in Eqs. (2) and (3), respectively.

$$\rho \frac{\partial u_i}{\partial x_i} = 0 \tag{2}$$

$$\frac{\partial}{\partial t}\rho\bar{u}_i + \frac{\partial}{\partial x_j}\rho\bar{u}_i\bar{u}_j = -\frac{\partial P}{\partial x_i} + \frac{\partial}{\partial x_j}\left[\mu\,\frac{\partial \bar{u}_i}{\partial x_j} - \left(\rho\overline{u'_i u'_j}\right)\right] \tag{3}$$

The turbulence model of Shear Stress Transport (SST) k-ω is implemented to calculate the unsolved Reynolds stress $\left(\rho\overline{u'_i u'_j}\right)$ term [10]. Since the k-ω SST features from k-ω and k-ε [11, 12], this model acts as k-ε in the free stream. But at the near wall region, this model can capture flow detail from the benefits of k-ω.

The force acting on the blade can be separated into lift and drag [13] that can be conducted to achieve propulsive force and torque as presented in Eqs. (4)–(6), respectively.

$$F_Y = F_{rel} sin\,\Theta \tag{4}$$

$$F_x = F_{rel} cos\,\Theta \tag{5}$$

$$M_T = D_T R \tag{6}$$

where F_Y is lift, Frel is relative force occurring on the blade, F_x is the propulsive force, M_T is total torque from aerodynamic drag, D_T is total drag that resists the rotation of the rotor, and R is rotor radius.

IV. Result and Discussion

This article focused on the effect of pitch angle amplitudes of 25º, 35º, and 45º on aerodynamic loads namely lift, propulsive force, torque, and lift-to-torque ratio. The range of rotor speed to use in this study was 400–800 RPM. The results of this study were divided into 2 sections as follows: (i) The results of 2D CFD simulation validation and (ii) the results of pitch angle effect.

A. The Rusults of 2D CFD Simulation Validation

The validation was an important process for examining whether the results from the 2D CFD simulation technique are satisfactorily consistent with the experiment data to ensure that the simulation results of this study could be acceptable. The results from CFD simulation technique of this study were validated with the experimental data of Hu [4] as mentioned in Section II.A. For this validation

process, the variables as follows: (i) lift, (ii) propulsive force, and (iii) torque generated by a single rotor were figured out in the range of 300–800 RPM as shown in Fig. 8. The results showed that the lift and torque provided from CFD simulation of this study tended to be close with the experiment data with the average of percent error of 13.8%. However, the results of propulsive force were not very accurate, especially at the high RPM, with an average of percent error of 169.1%. The reason behind the high error of propulsive force (thrust) is possibly caused by the total error resulting from a combination of error of the vector of lift and drag. Furthermore, the tip loss occurring from wingtip vortex, which does not occur on 2D simulation, could be a significant factor. Additionally, the *k-ω* SST may not be the best model to capture the phenomenon of the rotor. In summary for this validation process, the results of the lift and torque were quite accurate. On the other hand, the results of the propulsive force were still high percent error.

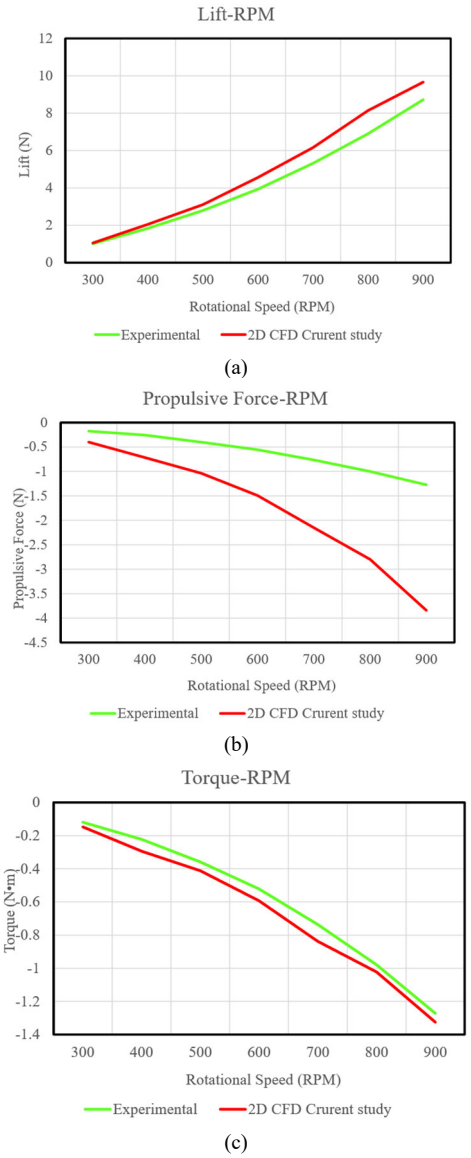

Fig. 8. The results between experiment and CFD simulation: (a) lift, (b) propulsive force, and (c) torque.

B. *The Results of Pitch Angle Effect*

As mentioned earlier, this article focused on the effect of pitch angle amplitudes of 25º, 35º, and 45º on aerodynamic loads namely lift, propulsive force, torque, and lift-to-torque ratio. The physical meaning of the lift-to-torque ratio refers to the mechanical advantage of a rotor operation of the cyclorotor. The 2-dimension CFD simulation technique was performed to estimate the results. The results of CFD simulation showed that the lift, propulsive force, torque, and lift-to-torque ratio were increased in higher rotation speed as depicted in Fig. 9. The pitch angle amplitude that provided the highest lift was, in order, 45º, 35º, and 25º as shown in Fig. 9(a). Additionally, the pitch angle amplitude that produced the maximum propulsive force was 25º, 35º, and 45º, respectively, as shown in Fig. 9(b). Furthermore, the pitch angle amplitude that offered the lowest torque was, in order, 25, 35, and 45 as shown in Fig. 9(c). Finally, the pitch angle amplitude that promoted the highest lift-to-torque ratio was 25º, 35º, and 45º, respectively, as shown in Fig. 9(d).

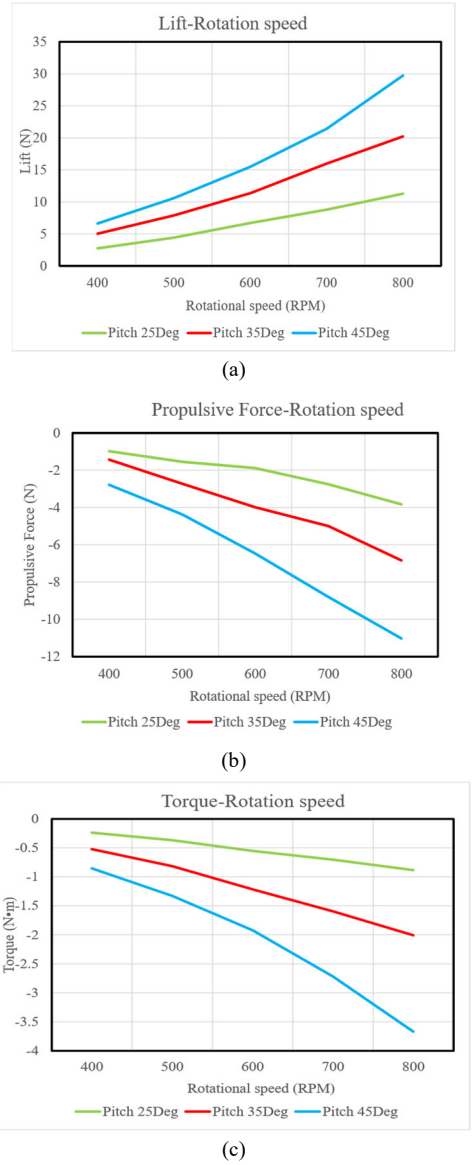

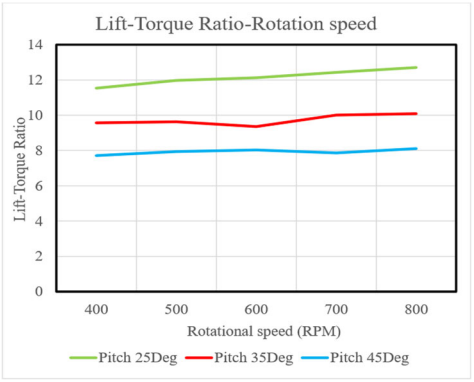

(d)

Fig. 9. The CFD simulation results of this study. (a) Lift; (b) Propulsive force; (c) Torque; (d) Lift-to-torque ratio.

In hovering state, the relative velocity of air flows through each cyclorotor blade in the direction of tangent to the circular trace. This flow causes the rotor to create a lift force in the normal direction and to create a drag force in opposite direction of rotation as depicted in Fig. 10. The lift forces generated by the blades at azimuth of 90º and 270º are constructive in vertical axis while the lift forces of the blades at azimuth of 0º and 180º would be destructive to each other in horizontal axis. The torque can be calculated from drag forces multiplied by radius of the rotor for all blades. The summation of the pressure difference between upper and lower surface of the airfoil blades in horizontal axis was close to zero because the pressure difference of the blades at the azimuth angle of 0º and 180º was on the opposite direction. On the other hand, the summation of the pressure difference between upper and lower surface of the airfoil blades in vertical axis was additive because the pressure difference of the blades at the azimuth angle of 90º and 270º was nearly the same direction as illustrated in Figs. A1(a), A2(a), and A3(a). However, the lift force (or lift) was the summation of pressure difference of all blades in vertical direction. The propulsive force was the resultant force in horizontal direction. The torque was the moment resisting to rotation of the rotor. The lift-to-torque ratio was the proportional of lift to torque. As mentioned in Section IV.B that the pitch angle amplitude of 45º provided the highest lift due to happening the most pressure difference in vertical axis as illustrated with the pressure contour in Figs. A4 (a), A5(a), and A6(a). In addition, for the propulsion force, it was obvious that all of three pitch angle amplitudes produced propulsion force nearly the same direction that was around the upper left corner of the domain as illustrated with the velocity field in Figs. A1(b), A2(b), and A3(b) including the vorticity field as shown in Figs. A4(b), A5(b), and A6(b) that show the low pressure region inside the rotor occurs from the vortex. Finally, for the torque, the pitch angle amplitude of 25º, which was the smallest one, offered the lowest torque because this amplitude was the utmost streamlined body of the rotor. Therefore, the drag force occurring that brought about the resistance to rotation (or torque) was lowest. The angle of attack (α) is an angle between chord line and the relative velocity of air. In hovering state, it is equal to the pitch angle. For the non-rotating flows over a 2D airfoil, an increase in the angle of attack results in an increase in both lift and drag force, up to a point, once the angle of attack is too high, lift force can be reduced rapidly due to the stall phenomenon, but the drag force still increases as shown in Fig. 11. The simulation results show that the pitch angle of 25º provide maximum the lift-to-torque ratio because this angle can generate the highest lift-to-drag ratio. In addition, since the stall delay phenomenon always occurs in rotating rotor devices, this causes the angle of attack of the cyclorotor providing maximum the lift-to-torque ratio is higher than the non-rotating flows providing maximum the lift-to-drag ratio (C_l/C_d). This was the reason why the maximum lift-to-drag ratio happened at the pitch angle amplitude of 25º as well.

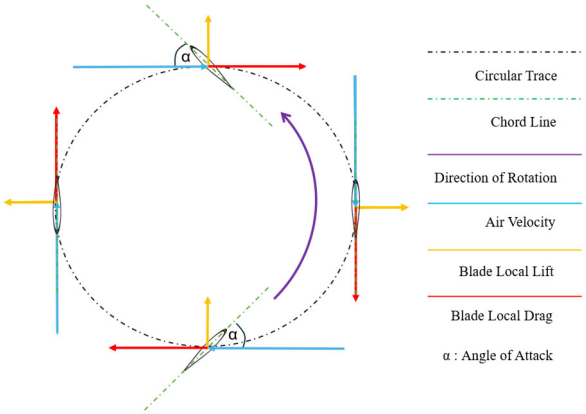

Fig. 10. Vector component of Force on the cyclorotor.

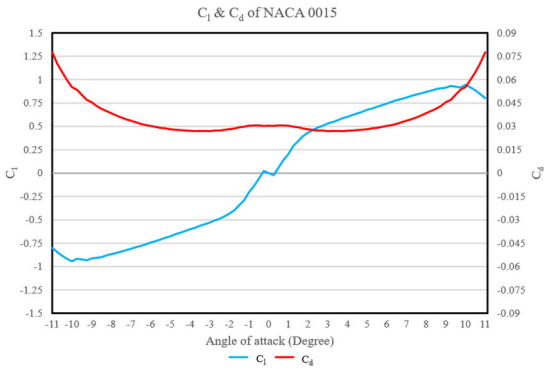

(a)

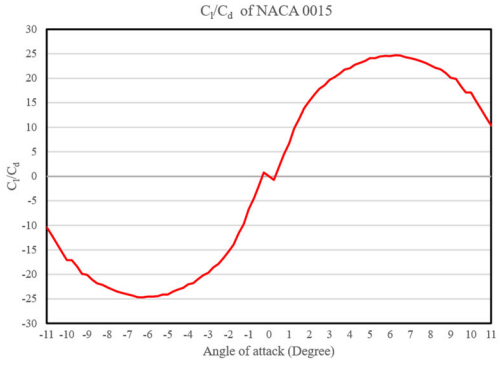

(b)

Fig. 11. (a) C_l, C_d and (b) C_l / C_d ratio of NACA0015 at Re = 50,000 [14].

V. Conclusion

The objective of this article is to study the effect of pitch angle amplitudes on the lift, propulsive force, torque, and lift-to-drag ratio by using the 2D computational fluid dynamics simulation. The variables of this study were as follows: the pitch angle amplitudes of 25º, 35º, 45º including the rotor speeds consisted of 400, 500, 600, 700, and 800 RPM. As a result, (i) The pitch angle amplitude of 45º provided the highest lift of 29.717 N at 800 RPM. (ii) The pitch angle amplitude of 45 degrees produced the maximum propulsive force of 11.026 N at 800 RPM. (iii) The pitch angle amplitude of 25 degrees offered the lowest torque of 0.239 N.m at 400 RPM. (iv) The pitch angle amplitude of 25 degrees promoted the highest lift-to-torque ratio of 12.705 at 800 RPM.

Appendix A Graphics of Flow Field

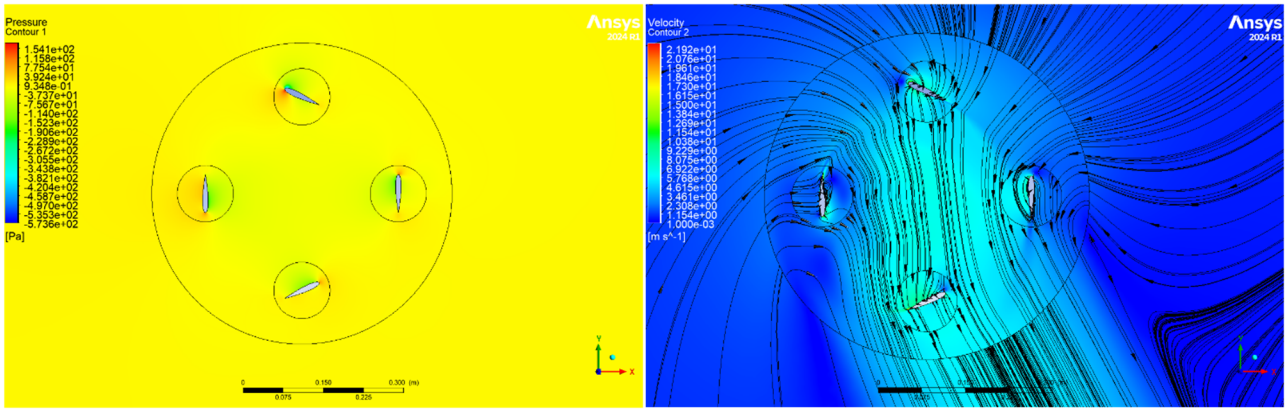

(a) (b)

Fig. A1. The results of (a) pressure contour and (b) velocity field for the pitch angle amplitude 25º at 800 RPM.

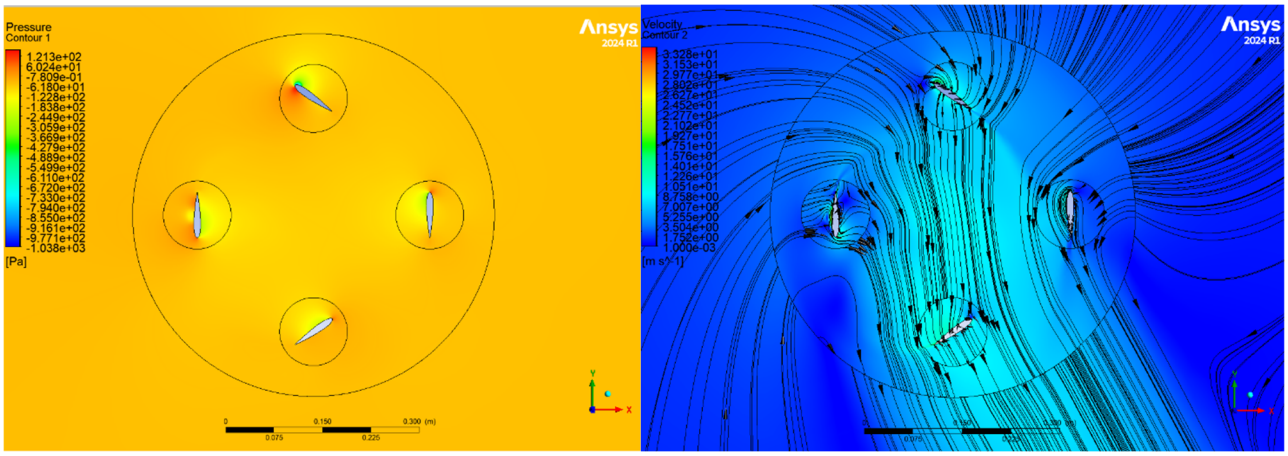

(a) (b)

Fig. A2. The results of (a) pressure contour and (b) velocity field for the pitch angle amplitude 35º at 800 RPM.

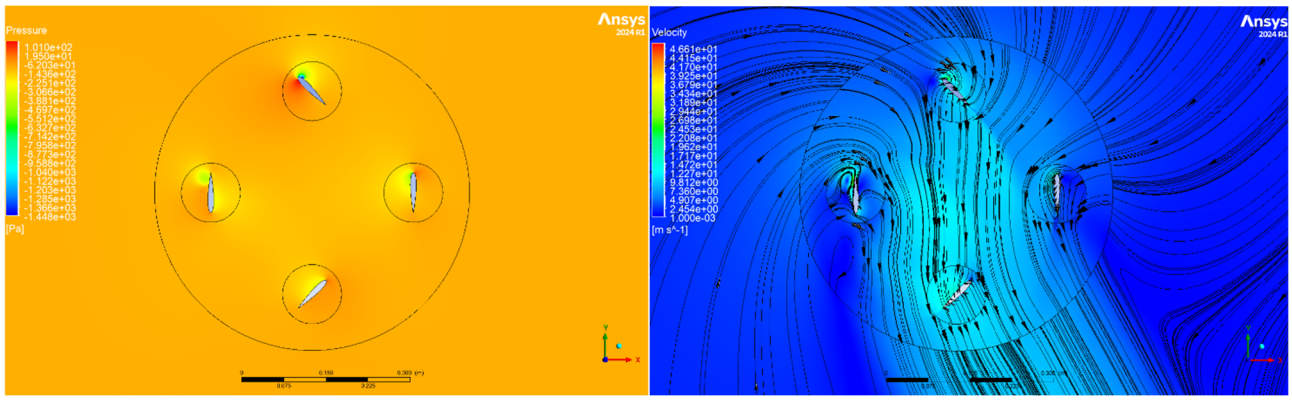

(a) (b)

Fig. A3. The results of (a) pressure contour and (b) velocity field for the pitch angle amplitude 45º at 800 RPM.

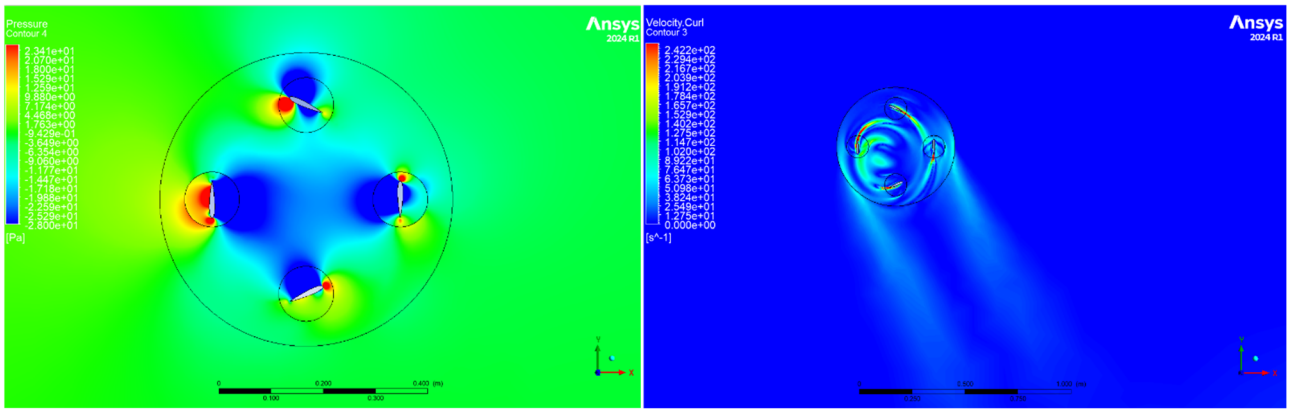

(a) (b)

Fig. A4. The results of (a) pressure contour and (b) vorticity field for the pitch angle amplitude 25º at 800 RPM.

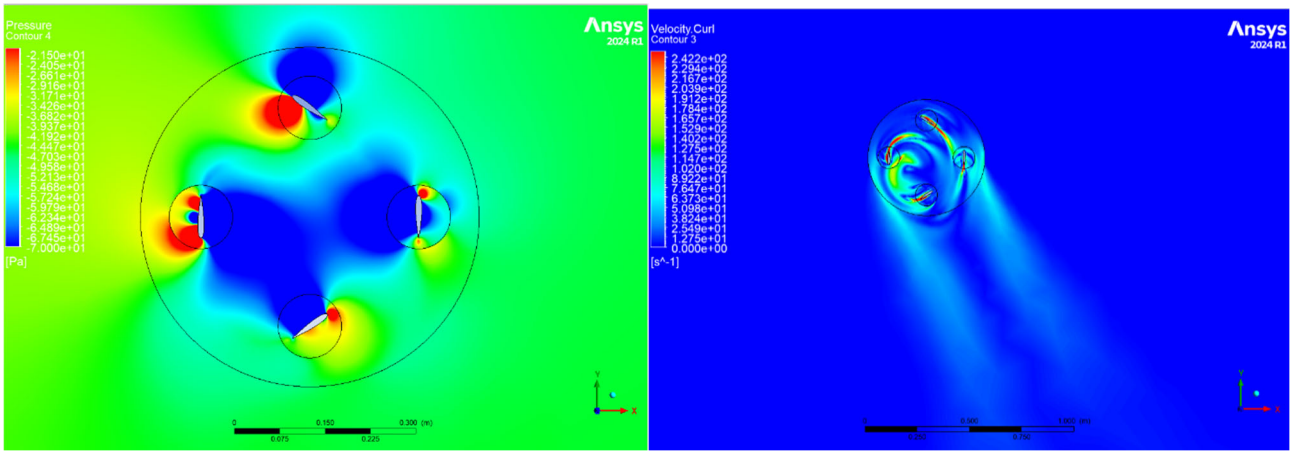

(a) (b)

Fig. A5. The results of (a) pressure contour and (b) vorticity field for the pitch angle amplitude 35º at 800 RPM.

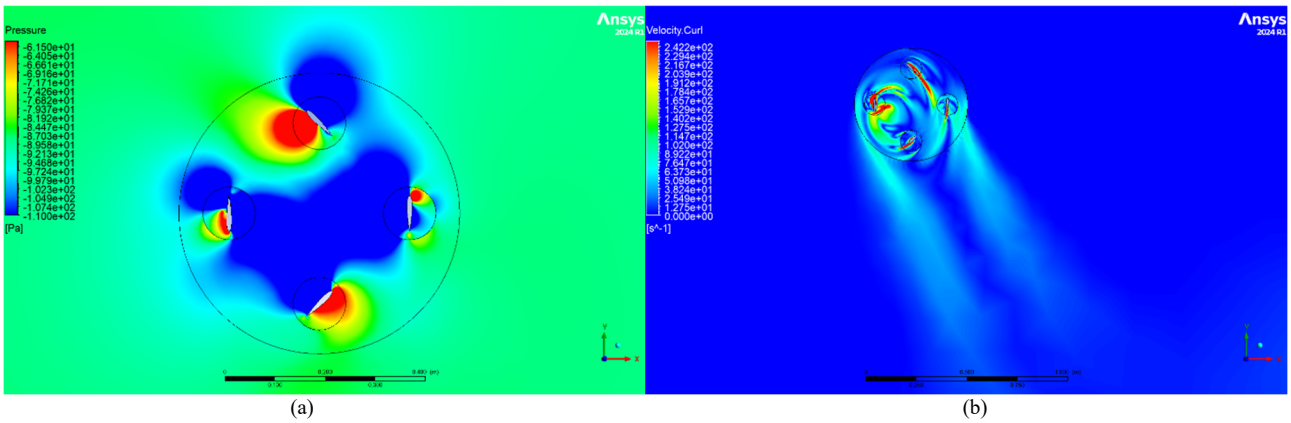

(a) (b)

Fig. A6. The results of (a) pressure contour and (b) vorticity field for the pitch angle amplitude 45º at 800 RPM.

Conflict of Interest

The authors declare no conflict of interest.

Author Contributions

Wishchayapas Piluck executed the CFD simulation process and analyzed all results. Kitsada Sangnak and Anasawee Arbubaka implemented the related literature survey and edited the article. Teerawat Klabklay provided advice throughout the study. All authors had approved the final version.

Funding

This research was funded by College of Industrial Technology, King Mongkut's University of Technology North Bangkok (Grant No. Res-CIT326/2023).

ACKNOWLEDGMENT

College of Industrial Technology, King Mongkut's University of Technology North Bangkok.

REFERENCES

[1] A. Benmoussa and J. C. Páscoa, "Cycloidal rotor coupled with DBD plasma actuators for performance improvement," *Aerosp. Sci. Technol.*, vol. 110, 106468, Mar. 2021. doi: 10.1016/j.ast.2020.106468

[2] M. Saito *et al.*, "Large-eddy simulation of blade-turbulence interaction in a cyclorotor system," *Aerosp. Sci. Technol.*, vol. 146, 108921, Mar. 2024. doi: 10.1016/j.ast.2024.108921

[3] Rotor Solutions. *Cyclotech*. [Online]. Available: https://www.cyclotech.at/rotor-solutions

[4] J. Hu *et al.*, "Numerical simulation to assess hydrodynamic performance of cycloidal propellers during maneuvering," *Ocean Eng.*, vol. 273, 113931, Apr. 2023. doi: 10.1016/j.oceaneng.2023.113931

[5] M. Habibnia and J. Pascoa, "ANN assisted flow modeling and analysis for a cyclorotor in ground effect," *Aerosp. Sci. Technol.*, vol. 95, 105495, Dec. 2019. doi: 10.1016/j.ast.2019.105495

[6] Y. Hu *et al.*, "Effects of blade aspect ratio and taper ratio on hovering performance of cycloidal rotor with large blade pitching amplitude," *Chin. J. Aeronaut.*, vol. 32, no. 5, pp. 1121–1135, May 2019. doi: 10.1016/j.cja.2019.01.015

[7] M. Saito and R. Ryoichi, "Numerical investigation of effects of blade-tip and number of blades in a cyclorotor system using large-eddy simulation," *Aerosp. Sci. Technol.*, vol. 158, 109951, Mar. 2025. doi: 10.1016/j.ast.2025.109951

[8] C. M. Xisto *et al.*, "Numerical modelling of geometrical effects in the performance of a cycloidal rotor," in *Proc. 11th World Conf. Comput. Mech.*, Barcelona, Spain, Jul. 2014. doi: 10.13140/2.1.1252.1600

[9] Q. Mo *et al.*, "Guidelines for the computational domain size on an urban-scale VAWT," in *Proc. Int. Conf. Mech. Eng., Intell. Manuf. Autom. Technol.*, Guilin, China, 2021. doi: 10.1088/1742-6596/1820/1/012177

[10] V. D. Narasimhamurthy. (2004). Unsteady-RANS simulation of turbulent trailing-edge flow. M.S. thesis, Dept. Thermo Fluid Dyn., Chalmers Univ. Technol., Goteborg, Sweden. [Online]. Available: http://tfd.chalmers.se/~lada/postscript_files/thesis_vagesh.pdf

[11] T. Li and S. Sun, "Numerical study on the scale effects of two-dimensional cycloidal propellers," *Ocean Eng.*, vol. 279, 114445, Jul. 2023. doi: 10.1016/j.oceaneng.2023.114445

[12] Z. Liu *et al.*, "Study on thrust directional steadiness of a cyclorotor," *Ocean Eng.*, vol. 287, 115840, Nov. 2023. doi: 10.1016/j.oceaneng.2023.115840

[13] L. Shi *et al.*, "Analysis of flow-induced performance change of cycloidal rotors: Influence of pitching kinematic and chord-to-radius ratio," *Ocean Eng.*, vol. 263, 112382, Nov. 2022. doi: 10.1016/j.oceaneng.2022.112382

[14] NACA 0015 (naca0015-il). *Airfoil Tools*. [Online]. Available: http://airfoiltools.com/airfoil/details?airfoil=naca0015-il